Activated carbon as catalyst in wet oxidation of phenol: Effect of the oxidation reaction on the catalyst properties and stability

T. Cordero [a], J. Rodríguez-Mirasol [a,*], J. Bedia [a], S. Gomis [b],
P. Yustos [b], F. García-Ochoa [b], A. Santos [b]

[a] Department of Chemical Engineering, E.T.S.I. Industriales, Universidad de Málaga, 29071 Málaga, Spain
[b] Department of Chemical Engineering, Facultad CC. Químicas, Universidad Complutense de Madrid, 28048 Madrid, Spain

Abstract

Catalytic wet oxidation (CWO) of phenol has been carried out in a continuous three-phase reactor by using a commercial activated carbon (AC) as catalyst, feeding oxygen as gas phase and an aqueous solution 1000 ppm in phenol to the reactor. A stable catalyst under operation conditions is one of the main difficulties to pass up in the catalytic wet oxidation process, so the stability of the activated carbon with the time on stream (TOS) was investigated. To do this the phenol conversion change was analyzed with TOS and results were contrasted to the change of the physicochemical properties of the AC with the TOS. Gas adsorption/desorption, TPD, XPS and SEM measurements were applied to the AC taken from the reactor after several TOS values. A significant reduction of the micro-pore volume and BET surface area of the catalyst was observed with TOS. However, as reaction proceeded the external surface area and the total amount of oxygen surface group increased. Moreover, regeneration of the initial catalyst properties was done by washing with water saturated in oxygen, at the reaction conditions or by heating in N_2 atmosphere at 450, 700 and 900 °C. The total micro-pore volume and internal surface area of the catalyst were not recovered by the regeneration process, probably due to blockage of the narrow micropores by pyrolytic carbon produced during the first step of the wet oxidation process.

1. Introduction

The pollution caused by industrial wastewaters is becoming an item of increasing importance and more restrictive government regulations are being imposed to control this problem. The organic compounds refractory to biological oxidation are among these toxic compounds that industrial wastewaters often release to the aquatic environment. These group of pollutants includes PAHs, dyes, halogenated hydrocarbons, phenolic compounds, etc., that cannot be treated by conventional biological processes. Moreover, the concentration of these pollutants in wastewater makes recovering non-profitable and alternatives for their removal must be considered. The most cited methods are adsorption, usually employing activated carbon [1,2], and the oxidation of the pollutants being

these techniques selected depending on the nature and concentration of the pollutant. Oxidation technologies can be classified depending on the oxidizer agent as advance oxidation processes, AOPs, being the oxidant the $OH^\bullet$ radical [3,4], and wet air oxidation, WAO, that uses O_2 as oxidant [5,6].

Both methods allow oxidizing the refractory organic pollutants to CO_2 and short chain acids which are more amenable to biodegradation. The main drawback of the AOPs processes is the costs of the reactive (H_2O_2, O_3, UV) that produce the $OH^\bullet$ radical. On the other hand, the WAO processes require high temperatures and pressures, typically in the range 473–573 K and 7–15 MPa, respectively, which severely affects the economy of this technology [7,8]. To achieve the oxidation of organic effluents under milder conditions catalytic WAO processes using homogeneous [9] or heterogeneous catalysts [10,11] have been investigated. While homogeneous catalysts needs of a further step to recover the catalytic dissolved species the use of heterogeneous catalysts in the process of wet oxidation is an

* Corresponding author. Tel.: +34 952132886; fax: +34 952132886.
E-mail address: mirasol@uma.es (J. Rodríguez-Mirasol).

attractive possibility, having being the object of numerous studies in the last decades.

Oxidation catalysts most usually employed can be classified into two groups: noble metals (Ru [12–14], Pd and Pt [12,15,16]) and metallic oxides (Cu [17–20], Mn/Ce [12,21], V [22] and Zn [23,24]). Most of the heterogeneous catalysts employed so far were not stable enough in strongly corrosive reaction media. Therefore, the main problem to be solved for the application of the catalytic wet oxidation process at an industrial scale is the stability of the catalyst. Catalysts based on noble metals are expensive and suffer a quick deactivation by fouling due to the formation of a polymer at the catalyst surface [25,26]. Metallic oxides (copper oxide shows the highest activity) are deactivated by leaching of the active phase due to the acidification of the media with the oxidation progress [27,28]. Moreover this leaching introduces an additional toxicity in the media [29,30] so that a treatment is required to recover the mineral species leached from supports and/or active phases.

In the last decade activated carbons have found many applications as supporting materials for noble metal catalysts employed in fine chemistry and environmental [31,32] because of their stability in various reaction media and of the easiness of metal recovery by burning off. Moreover, the catalytic properties of the surface functional groups of activated carbon, that may be present originally or introduced by specific chemical modifications, causes that activated carbons act also as catalyst, per se, in gas or liquid phase oxidation reactions, with molecular oxygen as oxidizing agent [33–35]. Indeed, activated carbon without metal impregnation seems to be a promising catalyst for liquid phase oxidation in general and in the catalytic wet oxidation of refractory organic pollutants in particular while it is relatively cheap and stable in both acidic and alkaline environments and avoids the leaching problem. As example, AC without impregnation has been recently used successfully as catalyst in the wet oxidation of phenolic wastewaters [36–40]. The main problem for the use of AC as catalyst in the CWO is to prevent the burning off of the solid. Thus, temperature and oxygen pressure must be fixed in an adequate operation range.

A remarkable difference between the activated carbon and other heterogeneous catalysts used in the wet oxidation technology is the higher adsorption capacity of the activated carbons. As was noticed in previous works [39,41] the organic pollutant and the organic oxidation intermediates are adsorbed and oxidized at the activated carbon surface finding negligible the oxidation reaction in the liquid phase. Because the adsorption-reaction of the organic compounds takes place at the catalyst surface it is probable that the physicochemical properties of the activated carbon surface will change during the process and this modification will influence the AC catalytic behavior. However, in literature only the influence of the initial surface groups of the activated carbon in the activity and selectivity of several oxidation reactions in liquid phases has been investigated concluding that the mechanism of oxidation involves the quinone type groups on the carbon surface while carboxylic and lactones not play an essential role in the

oxidation reaction [33,35]. These authors have concluded that the activity of carbon catalysts is mainly dependent of surface area and microporosity, while the surface oxygen groups are involved in the selectivity.

Taking into account that the catalytic activity of the activated carbon is attributed to its catalyst surface and considering that the industrial implementation of the catalytic wet oxidation requires of a stable catalyst it is clear that the evolution of the physicochemical properties of the activated carbon surface is a key parameter that must be analyzed.

The objective of the present works is to examine the effects of the catalytic wet oxidation of phenol (chosen as pollutant) on the change of the properties of the activated carbon used as catalyst. A commercial activated carbon selected in a previous work [42] has been used and reaction conditions were set to the maximum temperature (160 °C) and oxygen pressure (16 bar) of the range used for the kinetic analysis showed elsewhere [39,41]. A three-phase fixed bed reactor (FBR) will be used to carry out the oxidation runs and the catalyst modifications will be examined as a function of the time on stream under reaction conditions. Besides, influence of the evolution of the AC porous structure and surface chemistry on the catalyst activity will be explored.

2. Experimental

A commercial activated carbon from Chemviron carbon (Industrial React FE01606A) has been used. The activated carbon before using in the catalytic runs has been named as C0, having a BET surface area of 745 m^2/g, a external surface area of 63 m^2/g and micro- and meso-pore volumes of 0.322 and 0.120 cm^3/g, respectively.

2.1. Catalytic runs

Oxidation runs have been carried out in a fixed bed reactor with concurrent up-flow of gas and liquid phases. The FBR reactor is made of a stainless steal tube 0.75 cm in internal diameter and 25 cm in length. The experimental set-up is schematically shown elsewhere [41,42]. A bed of catalyst pellets crushed to 0.65 mm in diameter was placed, employing catalyst weight (W) of 3.5 g. Non-porous glass spheres 1 mm in diameter were used at the reactor entrance if necessary. The reactor was placed in an oven with PID temperature controller (± 1 °C). Two different pre-heaters were used for the gas and liquid pipes to reach the fixed values as operational conditions.

A solution with phenol concentration (C_0 PhOH) of 1000 ppm at pHo of 3.5 was fed to the reactor at a liquid flow rate (Q_L) of 90 mL/h. Mass flow controllers were used for both gas and liquid phases. The reactor was kept at constant pressure ($P_{REACTOR}$) and temperature (T), being the temperature set to 160 °C. Oxygen pressure in the reactor was fixed to 16 bar with a backpressure valve, with an oxygen flow rate (Q_{O_2}) of 90 mL/min. The equilibrium for dissolved oxygen was reached at the reactor pressure and temperature conditions. Different experiments were carried out placing fresh catalyst in the fixed bed reactor and holding the solid different times in the

Table 1
Experimental conditions of the fixed bed reactor experiments and names of resulting samples

Runs	$P_{REACTOR}$ (bar)	T (°C)	TOS (h)	C_0 PhOH (mg/L)	W/Q_L (g min/mL)	Q_L (mL/h)	Q_{O_2} (mL/min)
C1	16	160	30	1000	2.33	90	90
C2	16	160	50	1000	2.33	90	90
C3	16	160	80	1000	2.33	90	90
C4	16	160	200	1000	2.33	90	90
C5	16	160	218	1000	2.33	90	90
C6	16	160	280	1000	2.33	90	90
C7	16	100	2	–	–	0	90
C8	16	160	2	0	2.33	90	90
C9	16	160	5	0	2.33	26	0
C10	16	160	5	0	2.33	26	90

reactor at the same temperature (160 °C) and oxygen pressure (16 bar) conditions. After each time on streams (TOS) the activated carbon was taken out from the bed reactor and characterized. A summary of the operational conditions of these runs (C1–C6) is given in Table 1.

2.2. Oxygen effect

To analyze the influence of the oxygen on the modification of fresh and aged activated carbons four additional experiments (C7–C10, summarized in Table 1) were carried out. In C7 run only an oxygen flow was fed to the reactor filled with fresh catalyst and the experiment was carried out at 100 °C for TOS = 2 h. After this time the activated carbon was taken out from the bed reactor and characterized. C8 run was carried out feeding acid water without phenol (pH 3.5) and oxygen gas to the reactor filled with fresh catalyst (160 °C and 16 bar) and the activated carbon was taken out from the bed reactor after TOS = 2 h and characterized.

C9 run was carried out placing an amount of 1 g of the catalyst obtained from run C6 in the reactor; acid water saturated in He without phenol was fed to the reactor at 160 °C and 16 bar. No oxygen gas was fed to the reactor in this run. After a TOS of 5 h the activated carbon was taken out from the bed reactor and characterized.

Last run, C10, was carried out at similar conditions than C9 (1 g of the catalyst obtained from run C6, was placed in the reactor) but in this experiment acid water saturated without phenol was fed concurrently to an oxygen gas flow to the reactor at 160 °C and 16 bar. After a TOS of 5 h the activated carbon was taken out from the bed reactor and characterized.

2.3. Analytical methods

Liquid samples were periodically drawn and analyzed. Phenol and organic compounds were identified and quantified by HPLC (Hewlett-Packard, mod. 1100) using a diode array detector (HP G1315A); a chromolith performance column (monolithic silica in rod form, RP-18e 100–4.6 mm) was used as stationary phase; a mixture of acetonitrile, water and a solution of 3.6 mM H_2SO_4 in the ratio 5/90/5 (v/v/v) was used as mobile phase. Flow rate of the mobile phase was 1 mL min^{-1} and the UV detector was used at wavelengths of 192, 210, and

244 nm. Organic acids were analyzed by ionic chromatography (Metrohm, mod. 761 Compact IC) using a conductivity detector; a column of anion suppression Metrosep ASUPP5 (25 cm long, 4 cm diameter) was used as the stationary phase and an aqueous solution of 3.2 mM Na_2CO_3 and 1 mM $NaHCO_3$ as the mobile phase, at a constant flow rate of 0.7 mL min^{-1}. Total organic carbon (TOC) values in the liquid phase were determined with a Shimadzu TOC–V CSH analyzer by oxidative combustion at 680 °C, using an infrared detector.

2.4. Characterization of the carbon samples

The porous structure of the activated carbons and catalysts was characterized by N_2 adsorption–desorption at 77 K, performed in an Omnisorp 100cx equipment (Coulter). Samples were previously outgassed during at least 8 h at 150 °C. From the N_2 isotherm, the apparent surface area (A_{BET}) was determined applying the BET equation [43], the micro-pore volume (V_t) and the external surface area (A_t) were calculated using the t-method [44] and the meso-pore volume (V_{meso}) was determined as the difference between adsorbed volume at a relative pressure of 0.95 and V_t [45–47]. The Horvath and Kawazoe method [48] was used to obtain the micro-pore size distribution and the Barrett-Joyner and Halenda (BJH) method [49] was employed to determine the meso-pore size distribution using the desorption data.

The surface chemistry of the samples was analyzed by temperature-programmed desorption (TPD) and X-ray photo-electron spectroscopy (XPS). TPD profiles were obtained with a custom quartz tubular reactor placed inside an electrical furnace. The samples were heated from room temperature up to 900 °C at a heating rate of 5 °C/min in a helium flow (200 cm^3 STP/min). The amounts of CO and CO_2 desorbed from the samples (approximately 0.1 g) were monitored with a NDIR-analyzer (Siemens, mod. ULTRAMAT 22). Partial TPD at intermediate temperature, 450 and 750 °C, have been carried out over C6 carbon in order to study the thermal desorption pathway and thermal regeneration possibilities of these carbons. The resulting carbons have been named C11 and C12, respectively; C6 with TPD at 900 °C is named C13. X-ray photoelectron spectroscopy (XPS) analyses of the samples were obtained using a 5700C model physical electronics apparatus with MgKα radiation (1253.6 eV). For the analysis of

the XPS peaks, the C 1s peak position was set at 284.5 eV and used as reference to position the other peaks [50]. The fitting of the XPS peaks was done by least squares using Gaussian–Lorentzian peak shapes [51,52].

3. Results and discussion

The evolution of the catalyst activity in the phenol conversion and mineralization with the time on stream is showed in Fig. 1. As can be seen, no phenol and TOC are initially detected at the reactor exit. The difference between phenol at the reactor entrance and reactor exit is due to both adsorption and oxidation and cannot be properly called ''phenol conversion'' in the sense that not all the phenol disappeared at this initial TOS has reacted (by oxidation). The time elapsed until phenol is detected at the reactor exit will depend on the reaction conditions [37] as well as the time required to reach a steady state operation where constant values for phenol conversion and mineralization are obtained with the time on stream. For the AC employed the time required to reach this steady state is about 50 h if a fresh activated carbon is placed in the reactor. The activated carbon recovered from the reactor had negligible weight changes (lower than 3%) in the time on stream range studied (0–280 h). This negligible lost of the catalyst mass means that AC here used has not been burned at the reaction conditions employed. The maximum oxygen pressure and temperature to avoid the burning off of the catalyst when activated carbon is used in wet oxidation process will depend on both the specific AC used and the equipment and operation employed. In this sense, if a three-phase fixed bed is used, the burning of the AC will happen easily if the reactor works in co-current up-flow (liquid and gas phases are fed from the reactor bottom). It is well known that a typical problem in trickle regime is the bad wetting of the catalyst. In this case, the oxygen gas phase can be directly in contact with the external AC surface producing a quicker burning of the catalyst. In up-flow operation, as is the case of this paper, the catalyst can be supposed being totally wetted by a liquid film, thus the oxygen is not burning the catalyst as easily as could be happen in a trickle operation. Most of the papers in literature studying the
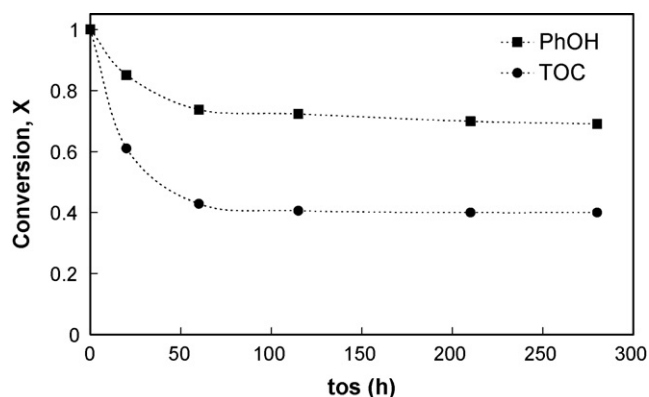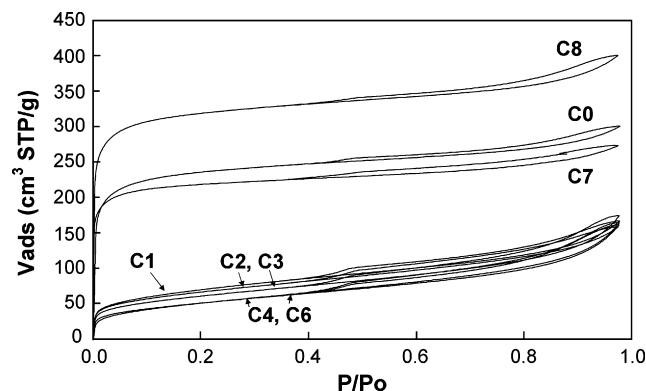

Fig. 2. N_2 adsorption–desorption isotherms of AC samples: fresh AC (C0), C0 after catalytic reaction at different TOS (C1–C6), C0 treated with oxygen (C7) and C0 treated with oxygen and water (C8).

catalytic wet oxidation of phenol with AC are carried out in fixed bed reactors working in trickle regime [37,53,54] but the possibility of a bad wetting of the catalyst is not analyzed.

To give explanation to the evolution of the catalyst activity in Fig. 1 (runs C1–C6) the changes on the surface area, pore size distribution and surface chemistry of the activated carbon with the time on stream have been analyzed. The aged activated carbon after each experiment has been denoted by the name of the corresponding run (i.e., C1–C8).

Fig. 2 shows the 77 K N_2 adsorption–desorption isotherms of the starting activated carbon C0 and the aged catalysts after the experiments of catalytic wet oxidation of phenol at different TOS (C1–C6). In order to study the effect of O_2 on the porous structure and surface chemistry of the catalyst, reaction with oxygen (C7) and with oxygen and acid water (C8) in the absence of phenol were carried out at similar conditions (see Section 2). The N_2 adsorption–desorption isotherms for the aged catalysts of these two experiments have been included in Fig. 2 for comparison. C0 activated carbon exhibits a type I isotherm, with high N_2 adsorption at low relative pressure and an almost plateau at high relative pressures, typical of microporous solids. The capillary condensation hysteresis observed at relative pressures higher than 0.4 suggests the presence of mesopores in the structure of this activated carbon.

When adsorption and oxidation of phenol take place simultaneously on the surface of the catalyst, an important reduction of the amount of N_2 adsorbed at low relative pressures and a slightly increase at high relative pressures is observed for the aged activated carbons (C1–C6), which is translated in a diminution of the apparent BET surface area and micro-pore volume and a little increase of the external area and meso-pore volume (Table 2). The significant reduction of the microporous structure of the catalyst is produced in the first step of the CWO reaction, at TOS values of 30 h.

The observed reduction of the micro-pore volume of the catalyst with reaction time may be attributed to phenol adsorption with oxidative coupling [55–58], molecular or dissociative oxygen chemisorption on the surface of the micro-pores entrance and/or to oxidation of phenol on the surface of the micro-pore entrance of the activated carbon with formation of stable oxygenated surface groups and pyrolytic carbon

Fig. 1. Phenol and TOC conversion as a function of time on stream. $T = 160$ °C, $W/Q_L = 2.3$ g_{cat}.min/mL, $PO_2 = 16$ bar, $Q_G = 90$ mL/min, $Co = 1000$ mg/L, and $pHo = 3.5$.

Table 2
BET and external surface areas and micro- and meso-pore volumes of the activated carbon before (C0) and after (C1–C8) been used as catalyst in the wet oxidation of phenol

Sample	A_{BET} (m^2/g)	A_t (m^2/g)	$V_t, d_p < 2$ nm (cm^3/g)	$V_{meso}, 2–50$ nm (cm^3/g)
C0	745	63	0.322	0.120
C1	356	105	0.122	0.158
C2	328	109	0.107	0.164
C3	328	112	0.107	0.168
C4	233	111	0.069	0.165
C5	249	113	0.070	0.163
C6	220	127	0.047	0.187
C7	714	60	0.310	0.110
C8	1048	76	0.477	0.114

Fig. 3. Micro-pore size distribution for C0, C7, C8 and some selected AC samples after phenol oxidation reaction (C3, C5 and C6).

deposition, blocking the narrower micropores during the first stage of the reaction. Once the steady state is reached the reaction occurs on the wide micropore and external area.

In order to verify the effect of oxygen on the surface of the activated carbon two experiments, previously described, have been carried out (Table 1), from which carbons C7 and C8 have been obtained. N_2 adsorption isotherms for these carbons appear also in Fig. 2 and the corresponding data for surface area and porosity are presented in Table 2. C7 carbon was obtained by treatment of C0 with O_2 in gas phase at 16 atm and 100 °C during 2 h without phenol. A slight reduction in the adsorption capacity of N_2 is observed for C7 carbon at low relative pressures, although the profile of the isotherm is very similar to that of C0 carbon, indicating a small reduction of the microporosity, with value of surface area very similar to that of C0. Sample C8 was produced by reacting C0 carbon with O_2 in acid water without phenol at 160 °C and 16 atm. An important increase of the N_2 adsorption at low relative pressure was observed for this carbon, which is traduced in an important increase in the BET surface area and the micro-pore volume (Table 2). Apparently, a partial gasification of the carbon has taken place at this operation conditions, causing the development of microporosity in C0. Other possible explanation is that leaching of the inorganic matter of the carbon may take place at this operation conditions, opening part of the porosity that could be blocked by the ash. Or, simply, the removal of the inorganic matter increases the surface area and pore volume just by elimination of mass that do not present porosity.

Fig. 3 shows the micro-pores size distribution for some selected samples. The C0 activated carbon shows a pore size distribution in the range of 1.4–1.8 nm (in diameter), with a maximum at 1.6 nm. When this activated carbon is treated with O_2 in the gas phase during 2 h (C7) a narrowing of the micro-pore structure is observed, with the maximum of the curve located now at 1.5 nm. This effect may be due to the dissociative chemisorption of O_2 on the surface of the micropores entrances. On the other hand, when C0 was treated in O_2 and acid water at 160 °C and 16 bar (C8) a slight widening of the micro-pore structure is observed, with the maximum peak centred now at slightly higher pore diameter. When the reaction of phenol oxidation takes place on C0 (C3,
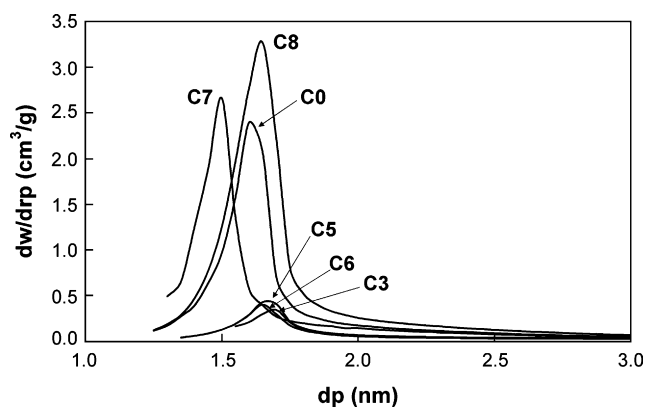
C5 and C6) only a small band can be observed in the pore size range of 1.56–1.76 nm (diameter), indicating that most of the narrowest micropores have disappeared with reaction (or have been blocked), remaining only a small proportion of the widest one of the original C0 activated carbon. These results suggest that the reduction observed in the surface area and the micro-pore volume of the fresh C0 is caused most probably by the adsorption and oxidation of phenol on the surface of the micropore entrance, blocking the narrow micropores with the formation of oxygen surface groups [56] and other carbon structures (pyrolytic carbon) coming from heterogeneous decomposition or cracking reaction [57,58].

TPD and XPS analysis of the carbon samples previously described have been performed in order to study the amount
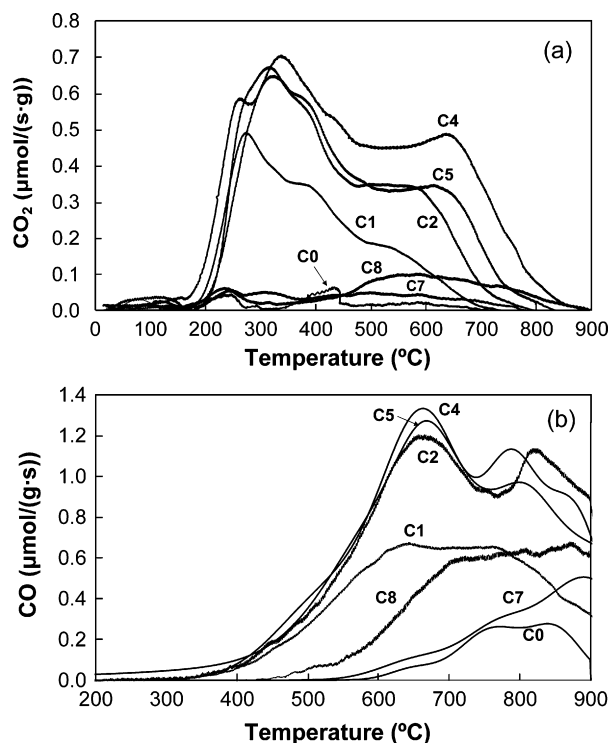

Fig. 4. TPD spectra of CO_2 (a) and CO (b) evolution from different AC samples (C0–C8).

and nature of the different surface oxygen complexes produced by the phenol oxidation reaction catalysed by carbon. Fig. 4 shows the TPD of the C0 starting activated carbon, the activated carbon obtained after the treatment in oxygen and in oxygen and acid water, both in the absence of phenol, C7 and C8, respectively, and different activated carbons obtained after several hours of phenol oxidation (C1, C2, C4 and C5). The evolution of CO_2 and CO with temperature provides an idea of the amount and type of oxygen surface groups, depending on their thermal stability. Very little amount of CO_2 (Fig. 4a) and CO (Fig. 4b) is observed as the temperature is increased for C0 carbon, which indicates the low concentration of oxygen complexes on the surface of this carbon. Carboxylic acid, anhydride and lactone type groups evolve as CO_2 and anhydride, phenol, carbonyl and quinone type groups desorb as CO upon thermal treatment [51,52].

The TPD of C7 activated carbon shows a slightly higher amount of CO desorbed at high temperatures than that of C0. The evolution of CO and CO_2 for C8 sample is somewhat higher than that for C7. However, this increase is not comparable to that observed for samples where the reaction of phenol oxidation has taken place. In this respect, an increase of TOS produces a progressive growth of the amount of oxygen surface complexes that evolve as CO_2 and CO during the TPD. Table 3 shows the amounts of CO_2 and CO released in the TPD experiments by the carbon catalyst after wet oxidation of phenol at different TOS, obtained by the integration of the areas under the TPD peaks. The amount of CO_2 and CO increases with the reaction time, reaching an almost steady state at TOS higher than 50 h, with amounts of CO_2 and CO of about 1.5 and 2.7 mmol/g of catalyst, respectively.

XPS analysis of the catalyst before and after the wet oxidation reaction provides an estimation of the chemical composition of the few uppermost layers of the catalyst and considers the superficial amounts of C and O atoms. The results have been included in Table 3 as C/O ratio value, which decreases with reaction time from 15.5 to a steady state value of approximately 6.7, supporting the finding derived from the TPD and N_2 adsorption experiments, i.e., the oxidation of the carbon surface upon phenol wet oxidation with formation of relatively stable oxygen surface complexes. This surface reaction reaches

a steady state at about 50 h, blocking the microporous structure of the catalyst.

The TPD peaks have been assigned to different types of oxygen surface groups depending on the desorption temperature [51,52,59]. The first CO_2 peak at around 250 °C may be attributed to carboxylic acid groups that present a low thermal stability. At higher temperatures lactone and carboxylic anhydride functions decompose forming also CO_2 ($\sim$400 and 650 °C, respectively). The CO TPD peaks observed at around 650, 780 and 840 °C originate from phenolic, carbonyl and quinone complexes desorption, respectively. Carboxylic anhydride groups decompose also as CO, at the same temperature as they do as CO_2. The TPD curves have been deconvoluted for the corresponding temperature peaks and the integration of the area under the deconvoluted TPD peaks provides the amounts of the different oxygen surface complexes (in mmol/g catalyst) on the surface of the catalyst before and after phenol wet oxidation.

Fig. 5 summarizes these data for the fresh and used catalysts (C0 to C6). For all the cases, the amount of oxygen surface groups increases with reaction time, reaching a steady state after 50 h of operation. At the steady state, the surface of the catalyst contains about 1 mmol/g of phenol, 0.7 mmol/g of carboxylic acid, 0.6 mmol/g of quinone, carbonyl and anhydride and 0.2 mmol/g of lactone. In a previous study, it was observed that phenol is oxidized to hydroquinone and catechol as first intermediates and these dyhydroxylbenzenes follow different oxidation routes producing benzoquinones and directly short chain acids and CO_2, respectively. p-hydroxybenzoic acid, which presented a slow oxidation rate, was also observed as an intermediate in the CWO of phenol. Fig. 5 suggests that the mechanism of phenol oxidation by activated carbon as catalyst involves not only the quinone type groups [33,35], but also phenolic, carboxylic acid, carbonyl and anhydride surface complexes, which seem to play an important role in the wet oxidation reaction.

In order to study the regeneration of the initial physico-chemical properties of the catalyst, the activated carbon obtained after phenol wet oxidation during 280 h, C6, has been treated in acid water saturated in He without phenol and without oxygen at 160 °C and 16 bar during 5 h. The catalyst thus obtained was denoted as C9. C10 carbon was obtained in

Table 3
XPS surface carbon/oxygen atomic concentration ratio and total amounts of CO_2 and CO released from TPD of fresh activated carbon (C0) and activated carbons used as catalyst

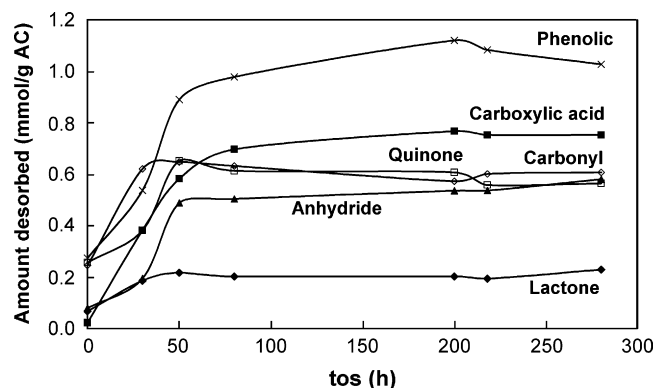| Sample	TOS (h)	C/O	CO_2 (mmol/g AC)	CO (mmol/g AC)
C0	0	15.48	0.171	0.857
C1	30	8.06	0.765	1.736
C2	50	6.47	1.289	2.679
C3	80	6.71	1.404	2.727
C4	200	6.73	1.484	2.779
C5	218	6.66	1.506	2.836
C6	280	6.04	1.564	2.910
C7	2	14.06	0.250	0.928
C8	2	9.07	0.159	1.165

Fig. 5. Amount of oxygenated functional groups (mmol of functional group/g AC) as a function of TOS, derived from the TPD experiments.
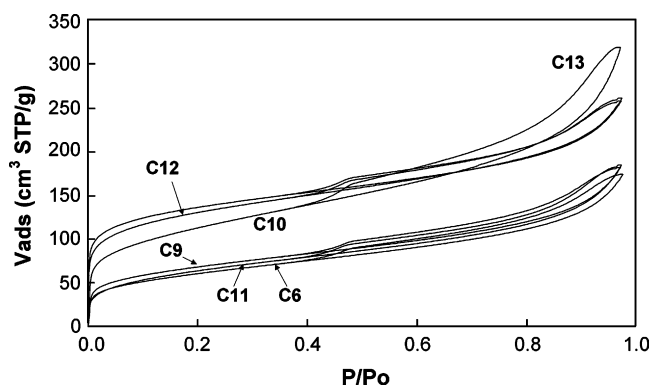
Fig. 6. N_2 adsorption-desorption isotherms of catalyst C6 and catalyst C6 after different regenerations treatments (C9–C13).
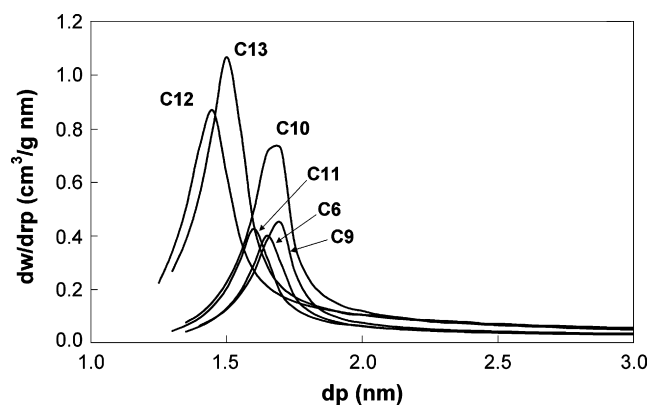

Fig. 7. Micro-pore size distribution of catalyst C6 and catalyst C6 after different regenerations treatments (C9–C13).

similar conditions as C9, but in this case an oxygen gas flow was fed concurrently to the acid water saturated without phenol.

N_2 adsorption-desorption isotherms at 77 K for C9 and C10 carbons are shown in Fig. 6. C6 isotherm has been included in this figure for comparison. Isotherm of C9 carbon is very similar to that of C6 carbon. Only a slightly increase of the N_2 adsorbed at low relative pressure is observed in the case of C9 isotherm. This treatment seems not to play an important role in the regeneration of the initial catalyst properties. However, the wet oxidation treatment seems to open the porous structure of the C6 carbon. C10 isotherm exhibits a higher adsorption of N_2 at low relative pressures and presents a more round knee, which extends up to increasingly higher relative pressures, characteristic of wide microporosity. The isotherm shows also a significant increase of the N_2 adsorbed at relative pressures higher than 0.4 and a larger hysteresis loop than C6, C9 and even C0 isotherms, indicating a considerable development of mesoporosity by the treatment with oxygen. Actually, C10 carbon presents the highest values of external surface area and meso-pore volume, 200 m^2/g and 0.333 cm^3/g, respectively (Table 4). However, this wet oxidation treatment did not recover the total surface area and micro-pore volume of the fresh C0 catalyst, which suggests that in these conditions wet oxidation is unable to remove the products of the decomposition (or the reaction intermediates) that partially block the micropores of the carbon. Figs. 7 and 8 represent the micro- and meso-pore size distributions, respectively, of different carbons. It is interesting to remark the wider micro- and meso-pore size distribution of C10 carbon with respect to C6 and C9. However, the maximum of both distribution curves remains at a constant pore size for the three carbons.

Fig. 9 represents the CO_2 and CO evolution from the TPD experiments for C6, C9 and C10 carbons. C9 treatment to C6 carbon slightly reduces the amount of CO_2 desorbed, especially at low temperature (<400 °C), that attributed to carboxylic acid surface groups, and substantially reduces the CO evolved at low and high temperatures, those ascribed to phenolic surface complexes, less stable and those corresponding to carbonyl and quinone surface groups, of higher thermal stability, respectively. It is interesting to point out that this regeneration treatment increases the amount of CO evolved at around 740 °C, which may originate from ether surface groups. This result suggests that treatment of C6 with acid water saturated in He without phenol and without oxygen slightly removes the less stable acid surface groups and eliminates almost completely the carbonyl and quinone surface groups and a large part of the phenolic functions. Part of the phenolic groups seems to produce, under this treatment, ether surface complexes [51]. Similar treatment conditions, but with the presence of oxygen gas flow (C10 run) produced a slightly reduction of the CO_2 and the CO evolved in the TPD experiment in the whole temperature range studied, with the exception of the CO desorbed at high temperature where a large reduction is observed, similar to that observed for C9 carbon. The presence of oxygen seems to avoid the formation of ether complexes from phenol groups.

Table 5 presents the amount of CO_2 and CO desorbed in the TPD experiments of C9 and C10 together with the C/O ratio obtained from the XPS analyses. Treatments C9 and C10 to C6 carbon reduced the amount of CO_2 and CO desorbed from the surface of the catalysts during the TPD experiments to values close to 1.02–1.5 mmol/g catalyst, respectively. The XPS C/O

Table 4

BET and external surface areas and micro- and meso-pore volumes of C6 catalyst after different regeneration treatments

Sample	T (°C)/$P_{REACTOR}$ (bar)/Regeneration agent	A_{BET} (m^2/g)	A_t (m^2/g)	V_t, $d_p < 2$ nm (cm^3/g)	V_{meso}, 2–50 nm (cm^3/g)
C9	160/16/He–water	257	111	0.072	0.184
C10	160/16/O_2–water	424	201	0.109	0.333
C11	450/1/N_2	246	120	0.059	0.197
C12	750/1/N_2	481	140	0.159	0.215
C13	900/1/N_2	499	146	0.171	0.221

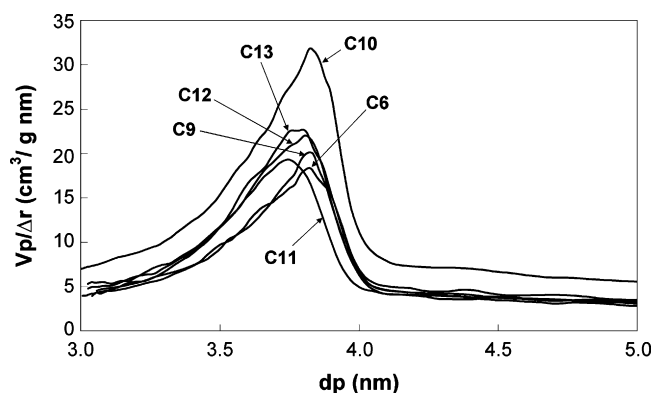Fig. 8. Meso-pore size distribution of catalyst C6 and catalyst C6 after different regenerations treatments (C9–C13).
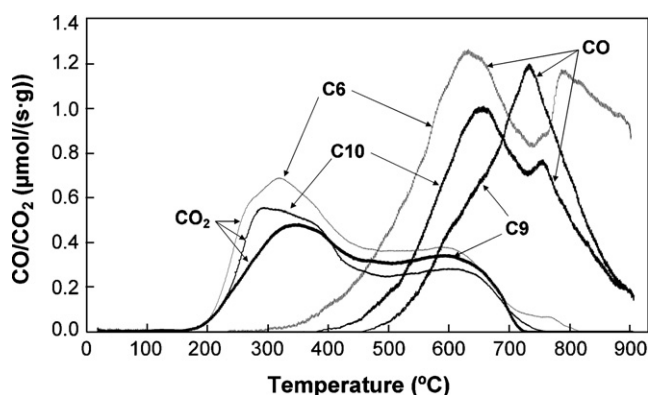

Fig. 9. TPD espectra of CO_2 and CO evolution from catalyst C6 and catalyst C6 after regeneration (C9 and C10).

ratio increases with these treatments from 6 to approximately 9, indicating also the elimination of oxygen from the surface of the catalyst. The values of the C/O ratio, of the amount of CO evolved from the TPD experiment (and in a less extent that of the CO_2) and of the apparent surface area for C6 carbon after the regeneration treatment C10 (i.e., C10 catalysts) are similar to those obtained after wet oxidation of phenol on the fresh catalyst during a TOS of about 30 h. These results indicate that this treatment, at the temperature, oxygen pressure and time interval studied (C10), regenerate only partially the surface of the aged catalysts, without reaching the original porosity and surface chemistry state of the fresh catalyst. This results is in agreement with the low CO_2 value obtained by analysing the

Table 5
XPS surface carbon/oxygen atomic concentration ratio and total amounts of CO_2 and CO released from TPD experiments of different samples

Sample	C/O	CO_2 (mmol/g AC)	CO (mmol/g AC)	mg CO_2 as C
C9	8.76	1.020	1.464	0
C10	9.08	1.025	1.536	≈3
C11	11.23	0.750	2.678	–
C12	14.62	0.045	1.143	–
C13	17.30	0.0	0.071	–

Values of column 5 correspond to CO_2 as C measured obtained by analysing the gas phase during the regeneration in the fixed bed reactor.

gas phase from reactor for C10 regeneration run, as showed in Table 5.

An additional regeneration process has been carried out by thermal treatment of the aged carbon and the evolution of the surface chemistry and porous structure of the treated catalyst has been studied. C6 carbon has been heated in N_2 atmosphere at 450, 750 and 900 °C at a heating rate of 5 °C/min in a helium flow of 200 cm^3 STP/min in the TPD system. After the final temperature was reached the carbons were cooled in a He flow and taken out from the TPD setup and characterized. The carbons thus obtained were named as C11, C12 and C13, respectively.

The N_2 adsorption–desorption isotherms for these carbons have been plotted in Fig. 6. Heat treatment of C6 at 450 °C eliminates the less stable acid oxygen surface groups, those corresponding to carboxylic acid (see Fig. 4a). This treatment seems not to affect the porous structure of the aged catalyst, given that the N_2 isotherm for C11 is very similar to that of C6 (Fig. 6). The apparent surface area, the external surface area and the micro- and meso-pore volume values obtained for C11 carbon are also quite comparable to those observed for C6 carbon (Tables 4 and 2, respectively). This result suggests that the carboxylic acid surface groups are formed during the wet oxidation of phenol on the very external surface of the catalyst.

The thermal treatment to C6 carbon at 750 °C produces a significant increase of the N_2 adsorbed at low relative pressures (see isotherm of C12 carbon in Fig. 6). However, the isotherm of the carbon obtained after the treatment at 750 °C, C12, is very similar to that of carbon C6 at relative pressures higher than 0.2, showing also the same hysteresis loop. The isotherm obtained for C13 sample, the carbon obtained after the heat treatment of the aged catalyst C6 at 900 °C, is very similar to that of C12 carbon, with slightly higher N_2 adsorption at relative pressure lower than 0.4. Table 5 presents the amount of CO_2 and CO evolved from the TPD and the C/O ratios obtained from XPS analysis of C11, C12 and C13 carbons. Thermal treatment at 750 °C removes almost completely (97%; see Tables 3 and 5) the oxygen surface complexes of C6 carbon that evolve as CO_2 in the TPD experiments, i.e., those corresponding to carboxylic acids, lactones and anhydrides. This treatment also eliminates about 60% (see also Tables 3 and 5) of surface complexes that evolve as CO at low temperatures, i.e., those ascribed to phenolic groups that present lower stability. Finally, the treatment at 900 °C eliminates almost completely the oxygen surface complexes from the surface of C6 and yields a XPS C/O ratio value of about 17 (Table 5), which is even higher that that obtained for the fresh catalyst C0. Very stable basic oxygen surface groups such as carbonyl and quinone are removed by the thermal treatment from 750 up to 900 °C.

These results suggest that mainly the phenolic surface complexes and, in some extent, the carboxylic acids and anhydrides formed on the surface of the catalyst during the phenol wet oxidation are responsible of the reduction of the internal surface area (and activity) of the original catalyst. Elimination of these oxygen surface groups by thermal treatment at 750 °C leads to the recovering of part of the

internal surface area and micro-pore volume of the aged catalyst (from 220 m^2/g in C6 to 480 m^2/g in C12 carbon). However, this regeneration treatment (and none of the other used in this study) could not recover the total internal surface area and micro-pore volume of the fresh catalyst C0 (745 m^2/g and 0.322 cm^3/g), which suggests that during the initial wet oxidation process phenol chemisorbs on the internal surface of the catalyst and decomposes under the operation condition used in this work, forming products (probably pyrolytic carbon) that partially block the microporous structure of the catalyst. These formed products are stable enough and cannot be removed by any of the regeneration treatments studied in this work.

It has to be mentioned that the activity of the catalyst remains high enough at the steady state (70% conversion; Fig. 1) given that the wet phenol oxidation process on the activated carbon produces an increase of the external surface area (from 63 m^2/g for C0 to 127 m^2/g for C6 carbon) and of the oxygen surface complexes that seem to be active for this reaction.

4. Conclusions

The commercial activated carbon used in this work, which does not contain metal active phase, presents a high catalytic activity and stability for the wet oxidation of phenol at the operation condition studied and avoids additional problems of deactivation or leaching of metal active phase. The catalyst shows an initial loss of activity with time on stream reaching a steady state phenol conversion of 70% and TOC of 40% at a time of reaction of about 50 h. The reduction of activity at the initial step can be attributed to a decrease of the micro-pore surface area of the catalyst. However, as reaction proceeded the external surface area and the total amount of oxygen surface group increased.

Regeneration of the initial catalyst properties was carried out by washing with water saturated in oxygen, at the reaction conditions or by heating in N_2 atmosphere at 450, 700 and 900 °C. The total micro-pore volume and internal surface area of the catalyst were not recovered by the regeneration processes, probably due to blockage of the narrow micropores by pyrolytic carbon produced during the first step of the wet oxidation process.

Acknowledgments

References

[1] T.C. Voice, in: H.M. Freeman (Ed.), Standard Handbook of Hazardous Waste Treatment and Disposal, McGraw-Hill, New York, 1997.

[2] D.Y. Tang, Z. Zheng, K. Lin, J.F. Luan, J.B. Zhang, J. Hazard. Mater. 143 (2007) 49–56.

[3] S. Esplugas, J. Giménez, S. Contreras, E. Pascual, M. Rodríguez, Water Res. 36 (2002) 1034–1042.

[4] H. Suty, C. De Traversay, M. Cost, Water Sci. Technol. 49 (2004) 227–233.

[5] H.M. Freeman, Standard Handbook of Hazardous Waste, McGraw-Hill, New York, 1997, Sections 8.6 and 8.11.

[6] F. Luck, Catal. Today 53 (1999) 81–91.

[7] S.T. Kolaczkowski, P. Plucinski, F.J. Beltrán, F.J. Rivas, D.B. McLurgh, Chem. Eng. J. 73 (1999) 143–160.

[8] H. Debellefontaine, J.N. Foussard, Waste Manage. 20 (2000) 15–25.

[9] D. Mantzavinos, R. Hellenbrand, A.G. Livingston, I.S. Metcalfe, Appl. Catal. B: Environ. 7 (1996) 379.

[10] Y.I. Matatov-Meytal, M. Sheintuch, Ind. Eng. Chem. Res. 37 (1998) 309–326.

[11] S. Imamura, Ind. Eng. Chem. Res. 38 (1999) 1743–1753.

[12] D. Duprez, J. Delanoë, J. Barbier, P. Isnard Jr., G. Blanchard, Catal. Today 29 (1996) 317–322.

[13] S. Imamura, I. Fukuda, S. Ishida, Ind. Eng. Chem. Res. 27 (1988) 718–721.

[14] J. Trawczynski, Carbon 41 (2003) 1515–1523.

[15] J.Y. Qin, Q.L. Zhang, K.T. Chuang, Appl. Catal. B: Environ. 29 (2001) 115–123.

[16] C.B. Maugans, A. Akgerman, Water Res. 37 (2003) 319–328.

[17] A. Sadana, J.R. Katzer, J. Catal. 35 (1974) 140–152.

[18] H. Ohta, S. Goto, H. Teshima, Ind. Eng. Chem. Fundam. 19 (1980) 180–185.

[19] A. Fortuny, C. Ferrer, C. Bengoa, J. Font, A. Fabregat, Catal. Today 24 (1995) 79–83.

[20] A. Santos, P. Yustos, B. Durban, F. García-Ochoa, Ind. Eng. Chem. Res. 40 (2001) 2773–2781.

[21] H. Chen, A. Sayari, A. Adnot, F. Larachi, Appl. Catal. B: Environ. 32 (2001) 195–204.

[22] Z. Ding, S.N.V.K. Aki, A. Abraham, Environ. Sci. Technol. 29 (1995) 2748–2753.

[23] A. Pintar, J. Levec, Chem. Eng. Sci. 47 (1992) 2395–2400.

[24] A. Pintar, J. Levec, Chem. Eng. Sci. 49 (1994) 4391–4407.

[25] S. Hamoudi, F. Larachi, A. Sayari, J. Catal. 177 (1998) 247–258.

[26] Z.P.G. Masende, B.F.M. Kuster, K.J. Ptasinski, F.J.J.G. Janssen, J.H.Y. Katima, J.C. Shouten, Appl. Catal. B: Environ. 41 (2003) 247–267.

[27] F. Arena, R. Giovenco, T. Torre, A. Venuto, A. Parmaliana, Appl. Catal. B: Environ. 45 (2003) 51–62.

[28] A. Santos, P. Yustos, A. Quintanilla, G. Ruiz, F. García-Ochoa, Appl. Catal. B: Environ. 61 (2005) 323–333.

[29] A. Santos, P. Yustos, A. Quintanilla, S. Rodríguez, F. García-Ochoa, Appl. Catal. B: Environ. 39 (2002) 97–113.

[30] A. Santos, P. Yustos, A. Quintanilla, F. García-Ochoa, Top. Catal. 33 (2005) 181–192.

[31] S.L. Cao, G.H. Chen, X.J. Hu, P.L. Yue, Catal. Today 88 (2003) 37–47.

[32] V.R. Gangwal, J. Van der Schaaf, B.F.M. Kuster, J. Catal. 232 (2005) 432–443.

[33] A. Pigamo, M. Besson, B. Blanc, P. Gallezot, A. Blackburn, O. Kozynchenko, S. Tennison, E. Crezee, F. Kapteijn, Carbon 40 (2002) 1267–1278.

[34] P. Korovchenko, C. Donze, P. Gallezot, B. Michèle, Catal. Today 121 (2007) 13–21.

[35] M. Besson, P. Gallezot, A. Perrard, C. Pinel, Catal. Today 102 (2005) 160–165.

[36] Y. Matsumura, T. Urase, K. Yamamoto, T. Nunoura, J. Supercrit. Fluids 22 (2002) 149–156.

[37] M.E. Suarez-Ojeda, F. Stuber, A. Fortuny, A. Fabregat, J. Carrera, J. Font, Appl. Catal. B: Environ. 58 (2005) 105–114.

[38] A. Santos, P. Yustos, S. Rodríguez, F. García-Ochoa, M. Gracia, Ind. Eng. Chem. Res. 46 (2007) 2423–2427.

[39] A. Santos, P. Yustos, S. Gomis, G. Ruiz, F. García-Ochoa, Chem. Eng. Sci. 61 (2006) 2457–2467.

[40] A. Santos, P. Yustos, S. Rodríguez, F. García-Ochoa, Appl. Catal. B: Environ. 65 (2006) 269–281.

[41] A. Santos, P. Yustos, S. Gomis, G. Ruiz, F. García-Ochoa, Ind. Eng. Chem. Res. 44 (2005) 3869–3878.

[42] A. Santos, P. Yustos, T. Cordero, S. Gomis, S. Rodríguez, F. García-Ochoa, Catal. Today 102 (2005) 213–218.

[43] S. Brunauer, P.H. Emmett, E. Teller, J. Am. Chem. Soc. 60 (1938) 309–319.

[44] B.C. Lippens, J.H. de Boer, J. Catal. 4 (1965) 319–323.

[45] S.I. Gregg, K.S.W. Sing, Adsorption, Surface Area and Porosity, Academic Press, London, 1982.

[46] J. Rodríguez Mirasol, T. Cordero, J.J. Rodríguez, Energy Fuels 7 (1993) 133–139.

[47] E. González Serrano, T. Cordero, J. Rodríguez Mirasol, J.J. Rodríguez, Ind. Eng. Chem. Res. 36 (1997) 4832–4838.

[48] G. Horvath, K. Kawazoe, J. Chem. Eng. Jpn. 16 (1883) 470–475.

[49] E.P. Barret, L.G. Joyner, P.P. Halenda, J. Am. Chem. Soc. 73 (1951) 373–380.

[50] S. Biniak, G. Szymanski, J. Siedlewski, A. Swiatkowski, Carbon 35 (1997) 1799–1810.

[51] J.L. Figueiredo, M.F.R. Pereira, J.J.M. Órfao, Carbon 37 (1999) 1379–1389.

[52] T. Cordero, J. Rodríguez-Mirasol, N. Tancredi, J. Piriz, G. Vivo, J.J. Rodríguez, Ind. Eng. Chem. Res. 41 (2002) 6042–6049.

[53] A. Fortuny, J. Font, A. Fabregat, Appl. Catal. B: Environ. 19 (1998) 165–173.

[54] A. Quintanilla, J.A. Casas, J.J. Rodríguez, Appl. Catal. B: Environ. 76 (2007) 135–145.

[55] V.D. Mundale, H.S. Joglekar, A. Kalam, J.B. Joshi, Can. J. Chem. Eng. 69 (1991) 1149–1159.

[56] T.M. Grant, C.J. King, Ind. Eng. Chem. Res. 29 (1990) 264–271.

[57] R.D. Vidic, M.T. Suidan, R.C. Brenner, Environ. Sci. Technol. 27 (1993) 2079–2085.

[58] P. Magne, P.L. Walter, Carbon 24 (1986) 101–107.

[59] U. Zielke, K.J. Hüttinguer, W.P. Hoffman, Carbon 34 (1996) 983–989.